Available online at www.sciencedirect.com
SCIENCE DIRECT®
Environmental Pollution 127 (2004) 281–290
ENVIRONMENTAL POLLUTION
www.elsevier.com/locate/envpol

Exploring field vegetation reflectance as an indicator of soil contamination in river floodplains

L. Kooistra[a,b,*,1], E.A.L. Salas[c], J.G.P.W. Clevers[c], R. Wehrens[b], R.S.E.W. Leuven[a,1], P.H. Nienhuis[a,1], L.M.C. Buydens[b]

[a]*Department of Environmental Studies, University of Nijmegen, Toernooiveld 1, 6525 ED Nijmegen, The Netherlands*
[b]*Laboratory for Analytical Chemistry, University of Nijmegen, Toernooiveld 1, 6525 ED Nijmegen, The Netherlands*
[c]*Laboratory of Geo-information Science and Remote Sensing, Wageningen University and Research Centre, Droevendaalsesteeg 3, 6708 PB, Wageningen, The Netherlands*

Received 10 October 2002; accepted 10 July 2003

"Capsule": *Influence of elevated soil metal concentrations on field vegetation reflectance was assessed.*

Abstract

This study investigated the relation between vegetation reflectance and elevated concentrations of the metals Ni, Cd, Cu, Zn and Pb in river floodplain soils. High-resolution vegetation reflectance spectra in the visible to near-infrared (400–1350 nm) were obtained using a field radiometer. The relations were evaluated using simple linear regression in combination with two spectral vegetation indices: the Difference Vegetation Index (DVI) and the Red-Edge Position (REP). In addition, a multivariate regression approach using partial least squares (PLS) regression was adopted. The three methods achieved comparable results. The best R^2 values for the relation between metals concentrations and vegetation reflectance were obtained for grass vegetation and ranged from 0.50 to 0.73. Herbaceous species displayed a larger deviation from the established relationships, resulting in lower R^2 values and larger cross-validation errors. The results corroborate the potential of hyperspectral remote sensing to contribute to the survey of elevated metal concentrations in floodplain soils under grassland using the spectral response of the vegetation as an indicator. Additional constraints will, however, have to be taken into account, as results are resolution- and location-dependent.

Keywords: Heavy metals; Vegetation reflectance; Remote sensing; Multivariate statistics; River sediment

1. Introduction

Sediments deposited in floodplains along the rivers Rhine and Meuse in the Netherlands are characterized by elevated concentrations of metals (Middelkoop, 2000; Beurskens et al., 1994). Ecological risk assessment (Kooistra et al., 2001a) and soil sanitation (Schouten et al., 2000) require information on the spatial distribution of sediment quality in the floodplains. Without extensive and time-consuming fieldwork, it is often difficult to obtain an overview of the spatial distribution of contaminant concentrations. The application of remote sensing techniques offers potential advantages, such as synoptic information to characterize spatial and temporal heterogeneity and the possibility of measuring several floodplains simultaneously (Leuven et al., 2002).

For grassland that covers large areas of the Dutch river floodplains, the spatial distribution of contaminants may be inferred from diagnostic features in the spectrum of remotely sensed reflected radiation (Jago et al., 1999; Llewellyn et al., 2001). This assessment can be made because changes in the growing conditions of vegetation can induce modifications in biochemical composition (e.g. chlorophyll concentration), physiology and canopy architecture (Milton and Mouat, 1989). These modifications influence vegetation

* Corresponding author. Tel.: +31-317-464317; fax: +31-317-419000.
E-mail address: lammert.kooistra@wur.nl (L. Kooistra).
[1] Participants of Netherlands Center for River Studies (NCR), PO Box 177, 2600 MH, Delft, The Netherlands.

0269-7491/$ - see front matter © 2003 Elsevier Ltd. All rights reserved.
doi:10.1016/S0269-7491(03)00266-5

reflectance and can thus be used indirectly as an indicator of soil contamination. However, responses could be species-dependent, while geographical variations like soil type and the source of metal contamination also affect the relation between vegetation reflectance and metal concentrations (Horler et al., 1980).

A number of field studies have demonstrated that shifts in vegetation spectra were metal-induced due to geochemical stress (Kooistra et al., in press; Collins et al., 1983) or for old waste deposit sites (Lehmann et al., 1991; Sommer et al., 1998) and occurred in both the visible and the near-infrared (NIR) part of the spectrum. These studies used spectral vegetation indices (VIs) to investigate changes in plant stress due to soil contamination. A vegetation index combines two or more spectral bands to enhance the vegetative signal while minimizing background effects; they are commonly used to measure the sensitivity of vegetation to stress (Mohammed et al., 2000). As hyperspectral remote sensing images are increasingly becoming available (Green et al., 1998), further exploration of the increased number of spectral variables is a logical step. Multivariate statistical methods like partial least squares (PLS) regression are a promising approach to deal with large amounts of spectral information. Kooistra et al. (in press) tested both PLS and a total of 40 VIs for their correlation between elevated soil Zn concentrations and the reflectance of perennial ryegrass (*Lolium perenne*) in an experimental lysimeter set-up. The narrow band vegetation index MSAVI2mm and PLS gave a high classification accuracy for the strongly contaminated soil class, while the total accuracy was satisfactory. However, the validity of these relations in river floodplains under field conditions still needs to be explored.

This paper examines the relation between vegetation reflectance and different levels of soil metal concentrations for natural grasslands in contaminated river floodplains. High-resolution vegetation reflectance spectra were obtained using a field radiometer. Both simple regression with vegetation indices and a multivariate regression approach were adopted to evaluate this relation. Finally, we discuss the relevance of the established relations for management of contaminated floodplains and the critical factors for the application of remote sensing to assess various levels of contamination on the basis of vegetation reflectance.

2. Materials and methods

2.1. Site and sample locations

This study was carried out in the Afferdensche and Deestsche Waarden floodplain (250 ha) along the river Waal, the main branch of the river Rhine in the Netherlands (Fig. 1). A physical reconstruction plan for this area aims at the creation of more storage space for peak discharges in the river Rhine (Van der Perk, 1996). This is achieved by excavating a side-channel within the floodplain and by lowering the floodplain surface along this channel. Farmland within the floodplain is being transformed into wetlands, creating possibilities for ecological rehabilitation.

During the past decades, large amounts of contaminated sediment have been deposited in the floodplain by the Rhine, resulting in elevated metal concentrations in the soil (Middelkoop, 1997). Earlier studies of soil quality in the floodplain (Kooistra et al., 2001b) have revealed large spatial variability in soil metal concentrations. Low metal concentrations are sometimes found at a short distance from sites with relatively high contamination levels. As vegetation composition and coverage at this scale is relatively homogeneous and characterized by natural grasslands with patches of herbaceous vegetation, this gave us an opportunity to evaluate the effects of differences in soil metal concentrations on vegetation reflectance. The small-scale soil variation was taken into account by measuring vegetation reflectance along transects with measurements every 0.5 m.

In total nine georeferenced transects in areas with natural grassland were laid out in the floodplain (Fig. 1). Based on the locations of contaminated areas known from earlier studies (Kooistra et al., 2001b), most of the transects were located in areas with relatively high contamination levels. Three transects (6, 7 and 8) were positioned in an area that had recently been excavated, so relatively low soil metal concentrations were anticipated. Our selection of locations also took vegetation homogeneity into account, by choosing transects with comparable species composition and relatively high coverage. Detailed information on vegetation composition was available for three of the transects (Fig. 1).

2.2. Fieldwork and vegetation reflectance measurements

Field data were collected in the course of 3 days at the beginning of August 2001. For every 50 m transect, reflectance measurements were made every 0.5 m. A Fieldspec FR radiometer (Analytical Spectral Devices Inc., 1999) was used to measure vegetation reflectance spectra between 11:00 a.m. and 3:00 p.m., to ensure optimal sun conditions. The radiometer has a 25° field-of-view and the spectral bandwidth in the 400–2500 nm wavelength range is 1 nm. The fiber optic cable of the radiometer was mounted on a tripod at a height of 1 m in nadir position above the soil surface. This results in a circular field-of-view (FOV) with a diameter of 0.44 m and a ground surface area of 0.15 m^2. Before a reflectance spectrum was collected, a reflectance reference measurement with a standardized white spectralon

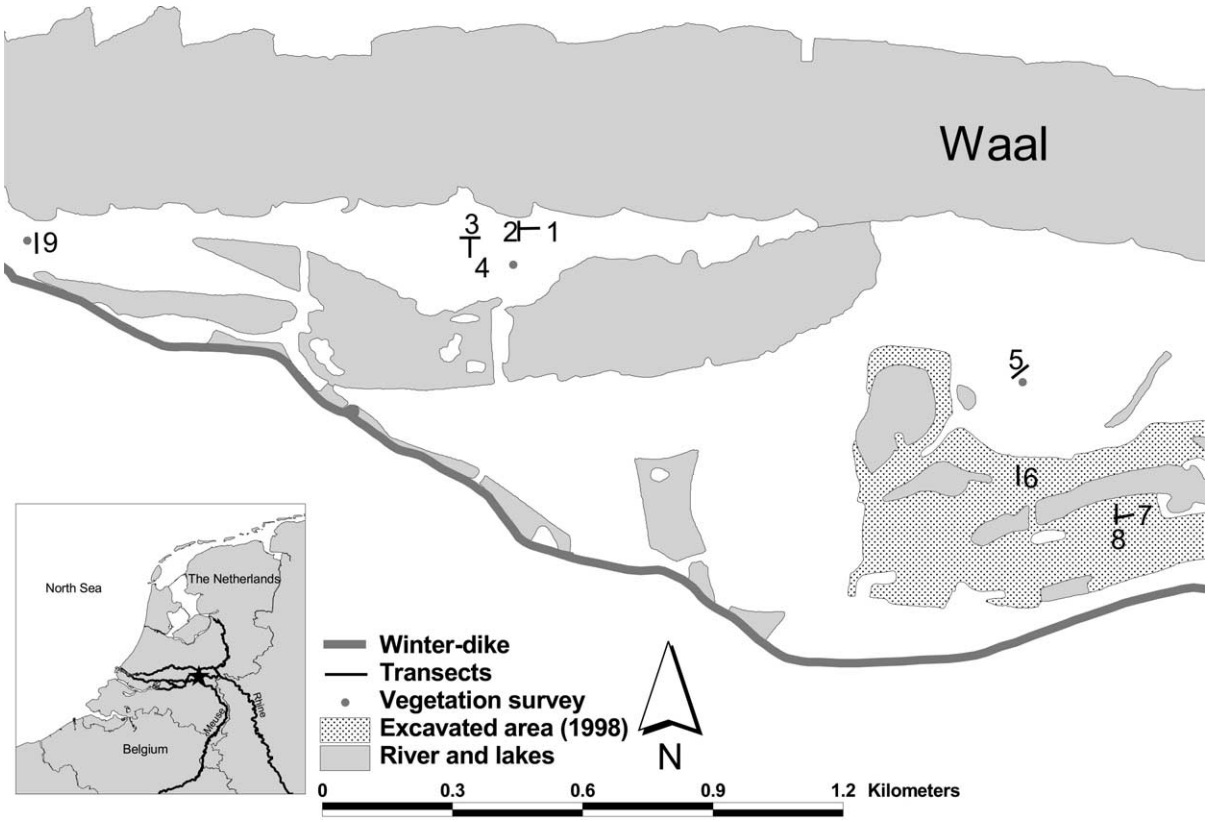

Fig. 1. Locations of the transects and main topographic features within the Afferdensche and Deestsche Waarden floodplain. The inset shows the location of the floodplain along the river Rhine in the Netherlands.

panel was made under the same conditions immediately before the target measurements. To reduce the noise level, every measurement was recorded as the average of 15 consecutively acquired spectra. The final conversion to spectral reflectance was done by dividing the radiance spectra of the vegetation samples by the radiance spectrum of the spectralon panel. A description of the vegetation within the FOV was made for every sampling point, including vegetation type and associated coverage. Six soil samples were collected along every transect, starting at 0 m and collecting a sample every 10 m. Samples consisted of three scoops from the top 10 cm of the soil within the FOV of the radiometer. The resulting 54 soil samples were stored in plastic bags, homogenized and taken to the laboratory for chemical analysis.

After removal of spectrally disturbed measurements caused by instrumental errors and atmospheric disturbances, the total data set for all nine transects consisted of 853 vegetation reflectance spectra. Only vegetation reflectance between 400 and 1350 nm was taken into account, because of absorption by atmospheric water vapor in the regions around 1400 and 1900 nm, and the relative high noise level in the spectra between 1900 and 2500 nm. A subset of 54 vegetation reflectance spectra was taken from the total set, corresponding with the locations for which soil samples had been taken. The vegetation reflectance curves for two of these samples were distorted due to an instrumental error. For these two samples, the reflectance measurement nearest to the soil sampling point (i.e., at a distance of 0.5 m) was used in the analysis.

2.3. Chemical analysis

Total metal concentrations for Ni, Cd, Cu, Zn and Pb in the soil samples were determined. Soil moisture and organic matter content were also determined, to evaluate the influence of additional soil parameters on vegetation reflectance. The moisture content of the soil samples was determined by oven-drying the soil samples at 105 °C for 24 h and measuring the weight loss. The organic matter content was obtained by a loss-on-ignition method (Houba et al., 1989). Oven-dried soil samples were put in the stove at 550 °C for 4 h. The organic matter content was calculated as the weight loss between samples dried at 105 and 550 °C divided by the dry weight of the soil sample.

The total metal concentration was determined by drying approximately 20 g of field-moist soil material at 105 °C for 24 h, grinding the dried soil material in a mortar and removing particles larger than 2 mm by sieving. Dried soil samples (1 g) were treated with a HNO_3/H_2O_2 solution in Teflon-lined bombs using the microwave digestion method; after mineralisation, total

metal concentrations were measured by means of ICP-AES spectrometry (Kooistra et al., 2001b).

2.4. Statistical analysis

Both the soil data and the total vegetation reflectance data set were analyzed individually using Principal Component Analysis (PCA) to identify relations between soil characteristics and to investigate the influence of species on vegetation reflectance, respectively. For the subset of 54 samples, the relationship between soil (contamination) parameters and vegetation reflectance was examined by means of two approaches. The first approach correlated spectral VIs and measured soil parameters and determined simple linear regression equations. In the second approach, multivariate statistical methods were examined.

The complete set of VIs presented by Kooistra et al. (in press) was evaluated for the present study, but this paper only reports the results for the two VIs that gave the best relationship (R^2) between metal concentrations and vegetation reflectance. These are the difference vegetation index (DVI) and the red-edge position (REP). The DVI can be characterized as a broad band VI and is calculated as the difference between the near-infrared (NIR) and the red band (Richardson and Everitt, 1992). The broad bands were calculated by simulating TM bands by spectral resampling of the measured spectra over the same waveband intervals as used by the Landsat TM sensor. The 630–690 nm and 760–900 nm intervals were used for the red and NIR bands, respectively. The REP is defined as the maximum slope of a vegetation reflectance spectrum between 690 and 740 nm (Miller et al., 1990), and was located by taking the maximum value of the first derivative of the vegetation reflectance spectrum within the red-edge region. This method requires detailed narrow band spectral information but is able to reveal fine details within the red-edge region (Llewellyn et al., 2001; Horler et al., 1983).

Partial least squares (PLS) regression has been extensively used as a multivariate quantitative technique in both soil (Reeves et al., 2002; Kooistra et al., 2001b) and vegetation analysis (Dury et al., 2001; Bolster et al., 1996). The PLS model can be used to identify relevant wavelength regions for the relationship being examined (Geladi, 2002). In the present study, the reflectance spectra were mean-centered and the number of PLS factors was determined by leave-one-out cross validation. Once the optimum number of PLS factors had been determined, a definitive model was developed. The criterion to add an additional factor to the model was that it had to reduce the root-mean-square error of cross validation (RMSECV) with $>2\%$. The RMSECV was calculated as the standard deviation of differences between the measured and predicted values determined from the regression models. Leave-one-out cross validation was also used to compare the various models. In addition, coefficients of determination (R^2) between measured and predicted values in the cross-validation were used to evaluate the relationships found. All calculations for the data analysis were written in Matlab™ (Mathworks Inc., 2001). Standard techniques were taken from the PLS-Toolbox for Matlab™.

3. Results

3.1. Analysis of soil properties

The results of the chemical analysis of the total Pb concentration and the organic matter content for all nine transects are shown in the boxplots of Fig. 2. The differences between the transects for the other metals showed the same trend as that observed for Pb, while organic matter represents the other soil properties. Transects 6, 7 and 8, located in the recently excavated area (Fig. 1), showed the lowest metal concentrations and organic matter contents, while the highest values were observed for transect 5. Organic matter content in transects 2 and 9, which are located near the river and perpendicular to it (Fig. 1), showed great variation within the transects, but the variation in soil properties between the transects was generally greater than that within the transects. The correlation matrix for all soil properties measured in the total sampling set is given in Table 1. A distinction can be made between the correlations among the various metals, which had values close to one, and the correlations between the metals and the organic matter and soil moisture content, which showed slightly lower but still significant ($P<0.005$) correlation values. The high correlation values among the metal concentrations indicate their common diffuse

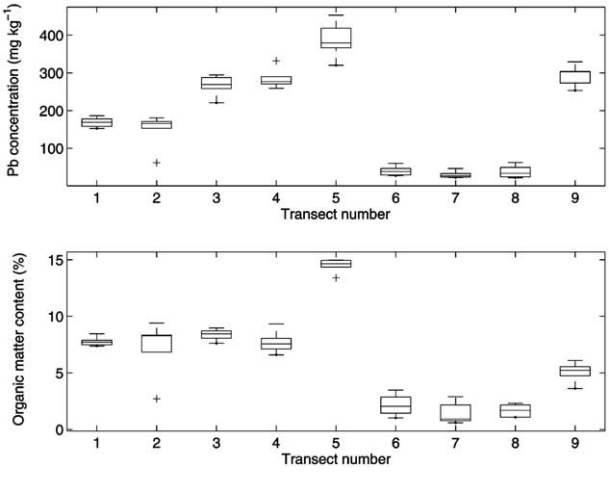

Fig. 2. Boxplots of Pb concentration and organic matter content for the nine transects in the the Afferdensche and Deestsche Waarden floodplain.

Table 1
Correlations between percentages of soil moisture, organic matter (OM) and metal concentrations (mg/kg) for the total sampling set of all nine transects ($n = 54$) in the floodplain Afferdensche and Deestsche Waarden

	Ni	Cd	Cu	Zn	Pb	OM	Moisture
Ni	1						
Cd	0.94	1					
Cu	0.97	0.99	1				
Zn	0.94	0.97	0.98	1			
Pb	0.95	0.99	0.99	0.99	1		
OM	0.96	0.88	0.91	0.87	0.87	1	
Moisture	0.91	0.81	0.84	0.80	0.81	0.91	1

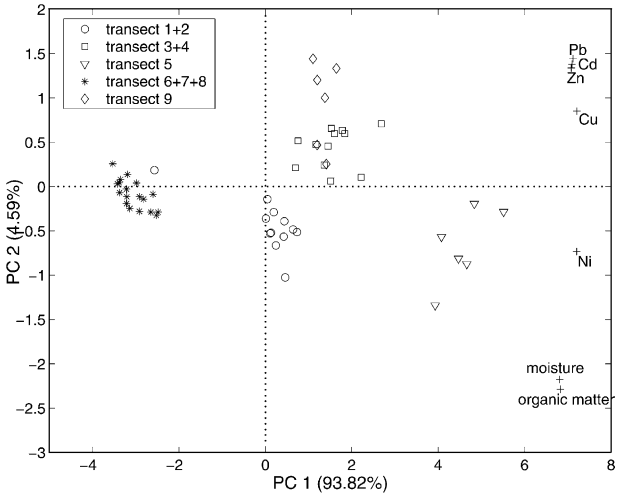

Fig. 3. Principal component analysis biplot of scores and loadings for the soil samples ($n = 54$) taken along the nine transects in the study area.

source (Middelkoop, 1997). The correlation between the metals and the organic matter content can be explained by the fact that the amounts of metals contained in the soil depend on the exchange capacity of the sediment particles, which is largely determined by the organic matter and clay content (Malley and Williams, 1997).

The PCA results for the auto-scaled soil properties of the sampling subset ($n = 54$) are shown in the biplot of Fig. 3. The biplot shows both the scores of the samples and the loadings of the soil variables in one figure. The first two principal components account for over 98% of the total variance. Apart from a few individual samples, a clear separation of most samples from the individual transects is observed. Although the first four transects were located in close proximity, the scores of transects 3 and 4 correspond more closely to that of transect 9. This can be explained by the fact that transects 1 and 2 were situated at a higher level in the landscape than transects 3, 4 and 9, resulting in a different flooding and sedimentation regime. The first principal component shows the general trend of the soil data with increasing PC1 scores for increasing values of the soil properties. The

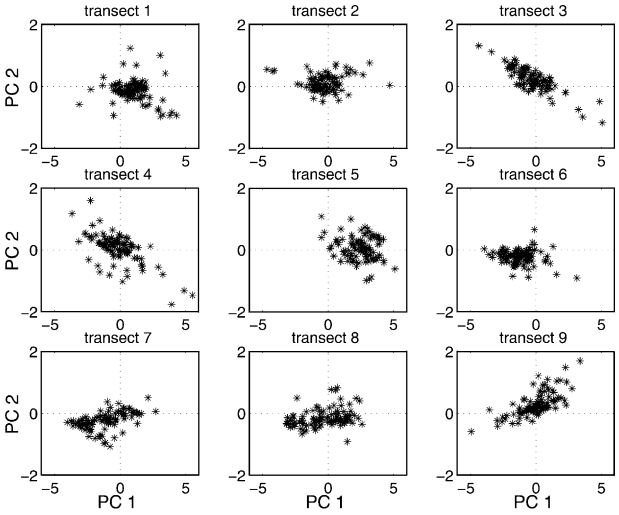

Fig. 4. Principal component analysis results for the total vegetation reflectance data set ($n = 853$). Scores for the nine transects are plotted in separate plots. The first principal component accounts for 92.6% of the total variance; the second principal component for 5.1%.

second principal component is related to the ratio between metal concentrations and the organic matter content. Samples with low PC2 scores had high metal concentration values but a relatively low organic matter content, while samples with a low metal–organic matter ratio had high PC2 scores. The loadings of the variables have comparable values for the first principal component. The second principal component separates the metals Cd, Zn, Pb, and Cu, which show a high correlation, from the organic matter and moisture content, while Ni has an intermediate loading value for PC2. The results of the biplot show that although Ni was closely correlated with the other metals (Table 1), it displayed a different kind of variation, which could be explained by a difference in source (Mohaupt et al., 2001).

3.2. Analysis of vegetation reflectance

The PCA results of the total mean-centered vegetation reflectance data set ($n = 853$) are shown for the individual transects in the scoreplots of Fig. 4. The first principal component for the total data set explains 92.6% of the total variance and is mainly related to the reflectance in the near-infrared region (700–1350 nm) of the spectra. The second component, which explains 5.1% of the total variance, shows high loading values around the red-edge region (700–800 nm) and in the 1150–1350 nm region. Although the scoreplot does not indicate a clear separation among the samples from the various transects, some differences between the transects can be observed. On the basis of the scores for PC1, a distinction can be made between transect 5, with high values, and transects 6, 7, and 8, with relatively low values. The scores for transects 1 and 2 are mainly concentrated in the center of the plot. The scores for transects 3, 4, and 9

show a relatively large variability in both PC1 and PC2, which could be related to the heterogeneous vegetation coverage in these transects.

The presence of different vegetation species within the FOV is an important explanatory factor for the variability in vegetation reflectance of a natural canopy. Differences in vegetation structure and architecture have a major influence on vegetation reflectance (Milton and Mouat, 1989). Fig. 5 presents the general trend of this influence for the area studied. The total data set of 853 reflectance spectra was divided into a set for which the coverage in the FOV mainly included grass species and a set for which the FOV was covered by more than 10% herbaceous species. Natural grassland not subject to intensive management contains large numbers of species. The main grass species in the area studied were *Poa annua* and *Lolium perene*. Within the grasslands, patches of rough herbaceous vegetation were found, dominated by *Urtica dioica*, *Cirsium arvensis* and *Rumex acetosa*. The upper plots in Fig. 5 show the scores of the PCA analysis as presented in Fig. 4, but with the scores classified on the basis of species type. Although there is some overlap between the score values at the center of the scoreplot, the grass samples are located mainly in the lower left part of the plot, while the samples with other vegetation are situated in the upper right part. The distinction between the two groups is mainly based on differences in score values for PC1. As for PC2, the rough vegetation samples tended to have a score larger than 0, while the scores for the grass samples varied over a wider range.

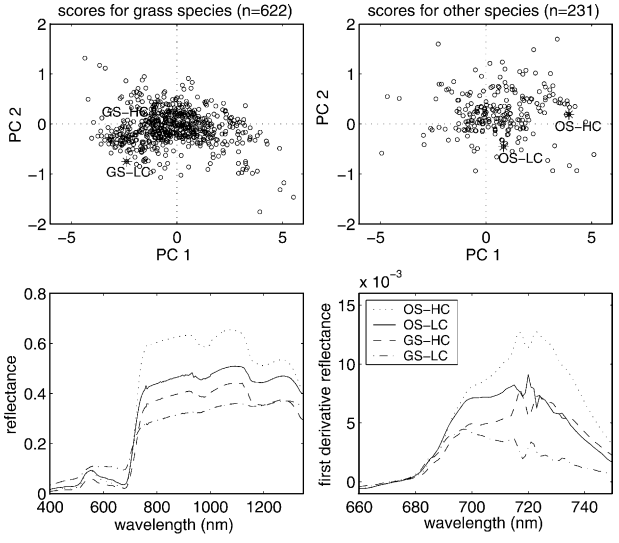

Fig. 5. Comparison of reflectance spectra for grass species and other species in the total data set. The upper two plots show the principal component analysis results with separate scores for grass samples and other vegetation samples. The lower plots show the reflectance spectra and the first derivative of the reflectance spectra for four selected samples from the scoreplots. The samples selected for this purpose are indicated by an asterisk in the scoreplots. OS other species, GS grass species, HC high contamination, LC low contamination.

The lower left plot in Fig. 5 shows four reflectance spectra that were selected from the scoreplots. The rough vegetation species showed high reflectance values in the near-infrared region (700–1350 nm), resulting in a high score value for PC1. The first derivative spectra in the lower right plot of Fig. 5 show that two maximum values can be identified within the red-edge region of the spectra: around 700 and 720 nm. The maximum around 700 nm is related to chlorophyll absorption, while the maximum around 720 nm is related to scattering within the leaf (Horler et al., 1983; Filella and Penuelas, 1994). The peak at 700 nm is more pronounced at lower vegetation coverage. With increasing coverage, resulting in more scattering within the leaf, the peak at 720 nm becomes more important and the peak at 700 nm is seen as a shoulder in the first derivative curve. On the basis of this we can state that the grass spectrum on the low contaminated site (GS-LC) has a relatively low vegetation coverage compared to the other spectra. From this, it was concluded that an assessment of the relation between soil properties and vegetation reflectance requires differences in species type to be taken into account.

3.3. Relation between soil metal contamination and vegetation reflectance

The relation between soil contamination and vegetation reflectance was evaluated on the basis of the subset of 54 samples for which soil properties were determined. A scatter plot of REP and DVI against Pb concentrations showed deviating values for the samples of transects 6, 7 and 8 (Fig. 6). The same trend was observed for the other metals and the organic matter and moisture content. These samples had all been taken in the area where the uppermost, clayey layer of the soil had been

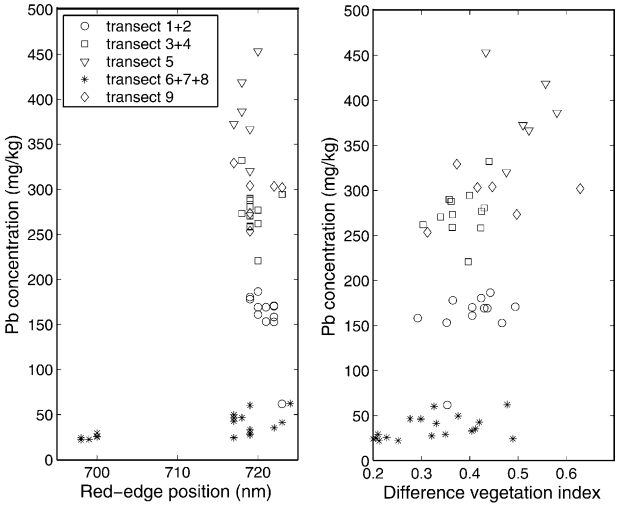

Fig. 6. Red-edge position (REP) and difference vegetation index (DVI) against Pb concentration for the vegetation reflectance subset for which soil samples were taken ($n = 54$).

removed down to the sandy basis. As a result of this recent excavation work, vegetation coverage was still low, while the contamination level was also considerably lower than in the other transects. It was therefore decided to exclude these samples from further analysis, resulting in a data set of 36 samples, of which 18 represented grass vegetation and the other 18 consisted of a mixture of rough vegetation and grass.

Table 2 presents the results of the methods evaluated to relate soil contamination and vegetation reflectance. A comparison of the grass set with the set including all vegetation samples showed a significant difference in RMSECV values ($P<0.1$). This is also reflected in the values for R^2, which were lower for the set with all vegetation samples. Fig. 7 shows that the herbaceous vegetation samples deviated considerably from the regression lines of the VIs with the Pb concentration and the organic matter content. Comparison of the three methods shows that, for the grass set, REP was not related to organic matter and moisture contents, while the R^2 value for the Ni concentration was also relatively low (Table 2). The DVI and PLS yielded lower cross-validation errors and relatively high R^2 values for these soil parameters. For the other metals and for the set with all vegetation samples, the results of the three methods were comparable.

The PLS models for both the grass set and the set with all vegetation samples required two factors. To improve our understanding of the functioning of the multivariate models, we examined the PLS regression coefficients (Fig. 8). The differences between the regression vectors for the soil parameters allowed a differentiation into two groups to be made, with organic matter, moisture content, and Ni in one group, and the other metals in the other. The regression vectors of the Pb concentration and organic matter content show that, although the general shape of the curves is comparable, there are a few areas with distinct differences (Fig. 8). The NIR region between 700 and 1100 nm was important for both soil parameters, while differences occurred in the regions around 550, 670, 1150, 1230, and 1270 nm.

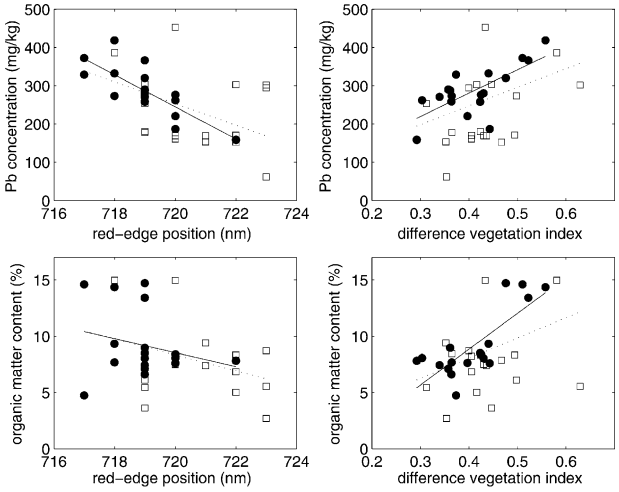

Fig. 7. Red-edge position (REP) and difference vegetation index (DVI) against Pb concentration and organic matter content for the set with grass samples (●) and the set with grass and other vegetation samples (□) but excluding the samples from the excavated area. The relationship for the grass samples ($n=18$) is indicated by the solid line, that for other vegetation samples ($n=36$) by the dotted line.

Table 2
Performance of the relationships between the examined vegetation indices and the measured soil parameters, compared with results of the multivariate PLS models for the set with grass samples and the set with all vegetation samples. In the second column the mean values for the soil parameters in the two sets are given. Comparison of the performance is based on the coefficient of determination (R^2) and the root-mean-square error of cross validation (RMSECV)

Soil parameter	Mean	DVI		REP		PLS	
		R^2	RMSECV	R^2	RMSECV	R^2	RMSECV
Grass samples (n = *18*)							
Ni (mg/kg)	90.3	0.73	9.4	0.23	16.2	0.72	10.4
Cd (mg/kg)	7.3	0.49	1.3	0.45	1.3	0.52	1.3
Cu (mg/kg)	143.5	0.57	22.4	0.51	24.0	0.58	24.4
Zn (mg/kg)	797.2	0.48	131.0	0.43	140.4	0.50	138.3
Pb (mg/kg)	281.9	0.50	49.6	0.61	39.1	0.51	53.1
Organic matter (%)	8.8	0.62	2.0	0.02	3.2	0.62	2.2
Moisture (%)	21.8	0.58	6.1	0.08	8.9	0.58	6.6
All vegetation samples (n = *36*)							
Ni (mg/kg)	85.8	0.22	17.9	0.27	17.0	0.31	19.9
Cd (mg/kg)	6.6	0.20	1.9	0.35	1.7	0.21	1.9
Cu (mg/kg)	129.6	0.18	37.0	0.37	32.8	0.20	39.4
Zn (mg/kg)	749.4	0.17	226.5	0.14	236.5	0.21	237.0
Pb (mg/kg)	257.4	0.19	80.9	0.29	76.7	0.21	84.6
Organic matter (%)	8.3	0.19	3.1	0.14	3.0	0.42	3.6
Moisture (%)	21.8	0.26	7.6	0.14	8.0	0.27	8.4

4. Discussion

4.1. Evaluating the validity of the established relations

The three methods for modeling the relationship between vegetation reflectance and metal contamination that we evaluated yielded comparable results (Table 2). Except for the relations between REP and organic matter and moisture content in the grass set, all R^2 values were significant ($P<0.05$). Earlier laboratory studies had already shown good results for the red-edge region as an indicator of vegetation stress caused by metal toxicity (Horler et al., 1980; Collins et al., 1983). A REP shift due to vegetation stress is often associated with a reduction in chlorophyll concentrations. Under field conditions, however, a mixture of distinct spectral components within the FOV can influence the peaks found in the first derivative spectrum (Llewellyn et al., 2001). The DVI combines the relatively insensitive red band with the more sensitive NIR region, which is influenced by vegetation morphology. Although vegetation stress may have affected light scattering in the NIR region as a result of differences in plant morphology, the results of the present study do not allow this effect to be attributed exclusively to metal toxicity. Fig. 7 shows that both REP and DVI yielded a cluster of points with relatively low metal concentrations deviating from the regression line. These points are located in transects 1 and 2 and have the lowest metal concentrations for the non-excavated area (Fig. 2). A possible explanation could be that a critical metal concentration has to be exceeded before metal toxicity occurs (Verkleij, 1994). In PLS, several wavelength regions seem to be important (Fig. 8), all of which, except for those around 550 and 670 nm, are located in the NIR region. The region around 550 nm could be related to chlorosis of the leaves (Adams et al., 1999).

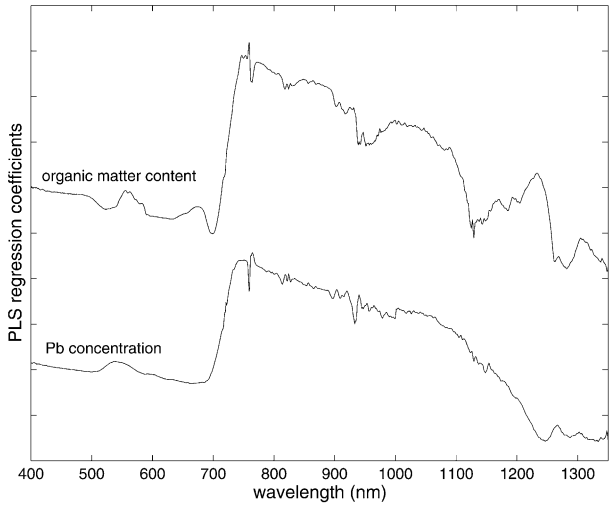

Fig. 8. Plot showing the regression vectors of the organic matter content and the Pb concentration for the PLS models of the subset, excluding the samples from the excavated area ($n=36$). Note that, for the sake of clarity, the individual plots have been given an offset.

The results of the present study suggest that the relationship between vegetation reflectance and soil metal contamination is species-dependent (Table 2). Herbaceous species showed a larger deviation from the relations established than grass species (Fig. 7). Possible explanations include differences in the structure of the vegetation and the morphology of the plant, which influence reflectance (Fig. 5), and differences in metal tolerance (Verkleij, 1994). The timing of data collection is another important factor. In a study by Bork et al. (1999), herbaceous vegetation types were best represented by June data, while grass vegetation was best classified by measurements made in August. In our study, data were collected in August, which could play a role in explain the finding that relationships for the grass species were better than those for herbaceous species. Hence, a proper application will require uniform vegetation coverage (Sommer et al., 1998). Although natural grasslands are relatively heterogeneous by nature, a possible strategy could be to divide the total area under investigation into relatively homogeneous vegetation sub-units, for which individual relationships are then derived.

4.2. Factors influencing the established relations

While the present study relates vegetation reflectance to total metal concentrations, toxic effects will mainly depend on the bio-available concentration of the metals. Bio-availability of metals in floodplains strongly depends on factors like pH and redox potential, which were not explicitly taken into account. Another aspect that needs to be considered is that soil samples were taken from the upper 10 cm. Roots of plants may penetrate deeper, and there is known to be considerable vertical variation in metal concentrations in floodplain soils (Middelkoop, 2000), with higher concentrations often found at depths greater than 10 cm. From this, it can be concluded that data in this study do not allow to distinguish the effects of metal toxicity from other disturbances like flooding, desiccation or nutrient deficiency. Additional parameters reflecting bio-available metal concentrations in soil and vegetation and physiological parameters such as chlorophyll would be required. However, the close correlation between the soil parameters in a fluvial environment (Table 1) could be utilized to make an indirect estimation of the contamination level. Instead of measuring the degree of plant stress, another option would therefore be to use differences in vegetation reflectance as an indicator of the presence or absence of stress (Miller et al., 1991). This information, with additional spatial data on measured point concentrations, soil and geomorphology within the floodplains, which are combined in geographical

information systems (GIS), could be used to assess contamination patterns.

A final point of consideration is the location-dependency of the results. Transferring the relationships derived here to other floodplains would require additional calibration data, as some factors are site-specific, e.g., main contaminant, dominant vegetation species, soil conditions. The effort required will depend on whether the aim is simply to assess the presence or absence of vegetation stress or whether the degree of stress is to be assessed as well. In addition, a distinction should be made between undisturbed floodplain soils and recently excavated areas (Fig. 6). This can be achieved by including spatial maps of recent floodplain reconstruction plans in the analysis.

Further research will be required to test the established relations in other river floodplains along the Rhine and Meuse and to assess their susceptibility to seasonal influences and increased levels of spectral noise. In addition, to evaluate the possibilities for general application of these relations for the Dutch river floodplains, an in-depth investigation is required into the causality of the relations that includes the acquisition of field information on the bio-availability and uptake of metals and its effect on plant physiology (e.g., chlorophyll) and on vegetation reflectance.

4.3. Application in operational remote sensing

A further step in the classification of contamination patterns in the Dutch river floodplains would be the use of images from airborne imaging spectrometers that give a fully synoptic overview of the area. Translating the results of the present field study with spectra measured at a point scale into image spectra recorded by an airborne sensor implies that a large number of additional factors and constraints have to be taken into account. The signal-to-noise ratio (SNR) of image spectra is usually significantly lower, while accurate radiometric and atmospheric correction is an important prerequisite (Kemper and Sommer, 2002).

The interpretation of the results of the present study also depends on both spectral and spatial resolutions. The spectral resolution of 1 nm acquired with the field radiometer is relatively large relative to that of the current hyperspectral sensors (at least 3 nm). The present study calculated REP on the basis of the maximum of the first derivative, a method that has the advantage of using all the information in the high-resolution reflectance spectra. Smoothing the reflectance spectra resulted in a detoriation of the relationship between REP and metal contamination. Apart from the spectral resolution, the spatial resolution is also an important factor. The FOV that was measured in this study with the radiometer was relatively small compared to that of currently used sensors (at least 5×5 m^2). Measuring a larger FOV will result in an averaging of the variation (Cutler and Curran, 1996) while the extracted pixel spectra could represent a mixture of different vegetation species. But as remote sensing images yield complete spatial coverage, this additional information could be included in the analysis to assess contamination patterns.

5. Conclusions

The results of the present study demonstrate the potential of remote sensing data to contribute to the survey of spatially distributed soil contaminants in floodplains under natural grassland, using the spectral response of the vegetation as an indicator. A satisfactory relationship was found for grass vegetation, with best R^2 values between predicted and measured concentrations for the metals ranging from 0.50 to 0.73. Herbaceous species displayed a larger deviation from the established relationships, resulting in lower R^2 values and higher cross-validation errors. From this we could conclude that these relations depend on species type and that future applications thus require a relatively uniform vegetation coverage.

Modeling the relationship between soil contamination and vegetation reflectance resulted in similar results for DVI, REP, and the multivariate approach using PLS regression. The data acquired in the present study did not allow the effects of metal toxicity to be distinguished from other stress effects. Additional research on the bio-availability of metals and the resulting plant uptake is recommended to explain the causality of the established relationships. It could be hypothesized that the close correlation between metal concentrations and soil parameters in a fluvial environment that affect water or nutrient deficiency (e.g., organic matter, clay) may be used to make an indirect estimation of the contamination level. The application of airborne remote sensing to assess contamination patterns will require additional factors and constraints to be taken into account, as the results of the present study are both resolution- and location-dependent.

Acknowledgements

The authors would like to thank Sander Wijnhoven for providing vegetation data and Jos Vink, Jan Klerkx and two anonymous reviewers for valuable comments on earlier versions of this paper.

References

Adams, M.L., Philpot, W.D., Norvell, W.A., 1999. Yellowness index: an application of spectral second derivatives to estimate chlorosis of leaves in stressed vegetation. International Journal of Remote Sensing 18, 3663–3675.

Analytical Spectral Devices Inc, 1999. Fieldspec FR: User's Guide. Analytical Spectral Devices Inc. (ASD), Boulder, Colorado, USA.

Beurskens, J.E.M., Winkels, H.J., Dewolf, J., Dekker, C.G.C., 1994. Trends of priority pollutants in the Rhine during the last 50 years. Water Science and Technology 29, 77–85.

Bolster, K.L., Martin, M.E., Aber, J.D., 1996. Determination of carbon fraction and nitrogen concentration in tree foliage by near infrared reflectance: a comparison of statistical methods. Canadian Journal of Forestry Research 26, 590–600.

Bork, E.W., West, N.E., Price, K.P., 1999. Calibration of broad- and narrow-band variables for rangeland cover component quantification. International Journal of Remote Sensing 18, 3641–3662.

Collins, W., Chang, S.H., Raines, G., Canney, F., Ashley, R., 1983. Airborne biogeophysical mapping of hidden mineral deposits. Economic Geology 78, 737–749.

Cutler, M.E.J., Curran, P.J., 1996. An observation of shifts in the position of the red edge at different spatial resoltions. In: RSS'96: Remote Sensing Science and Industry. Remote Sensing Society, Nottingham, pp. 290–297.

Dury, S., Turner, B., Foley, B., Wallis, I., 2001. The use of high spectral resolution remote sensing to determine leaf palatability of eucalypt trees for folivorous marsupials. International Journal of Applied Earth Observation and Geoinformation 3, 328–336.

Filella, I., Penuelas, J., 1994. The red edge position and shape indicators of plant chlorophyll content, biomass and hydric status. International Journal of Remote Sensing 15, 1459–1470.

Geladi, P., 2002. Some recent trends in the calibration literature. Chemometrics and Intelligent Laboratory Systems 60, 211–224.

Green, R.O., Eastwood, M.L., Sarture, C.M., Chrien, T.G., Aronsson, M., Chippendale, B.J., Faust, J.A., Pavri, B.E., Chovit, C.J., Solis, M.S., Olah, M.R., Williams, O., 1998. Imaging spectroscopy and the Airborne Visible Infrared Imaging Spectrometer (AVIRIS). Remote Sensing of Environment 65, 227–248.

Horler, D.N.H., Barber, J., Barringer, A.R., 1980. Effects of heavy metals on the absorbance and reflectance spectra of plants. International Journal of Remote Sensing 1, 121–136.

Horler, D.N.H., Dockray, M., Barber, J., 1983. The red edge of plant leaf reflectance. International Journal of Remote Sensing 4, 273–288.

Houba, V.J.G., Van der Lee, J.J., Novozamsky, I., Walinga, I., 1989. Soil and Plant Analysis, A Series of Syllabi. Part 5, Soil Analysis Procedures. Wageningen Agricultural University, The Netherlands.

Jago, R.A., Cutler, M.E.J., Curran, P.J., 1999. Estimating canopy chlorophyll concentration from field and airborne spectra. Remote Sensing of Environment 68, 217–224.

Kemper, T., Sommer, S., 2002. Estimate of heavy metal contamination in soils after a mining accident using reflectance spectroscopy. Environmental Science and Technology 36, 2742–2747.

Kooistra, L., Leuven, R.S.E.W., Wehrens, R., Nienhuis, P.H., Buydens, L.M.C., 2001a. A procedure for incorporating spatial variability in ecological risk assessment of Dutch river floodplains. Environmental Management 28, 359–373.

Kooistra, L., Wehrens, R., Leuven, R.S.E.W., Buydens, L.M.C., 2001b. Possibilities of VNIR spectroscopy for the assessment of soil contamination in river floodplains. Analytica Chemica Acta 446, 97–105.

Kooistra, L., Leuven, R.S.E.W., Wehrens, R., Nienhuis, P.H., Buydens, L.M.C. A comparison of methods to relate grass reflectance to soil metal contamination. International Journal of Remote Sensing 24 (in press).

Lehmann, F., Rothfuss, H., Werner K., 1991. Imaging spectroscopy data used for geological and environmental analysis in Europe. In: Summaries of the Third Annual JPL Airborne Geoscience Workshop, 20 and 21 May 1991. JPL, Pasadena, pp. 62–71.

Leuven, R.S.E.W., Poudevigne, I., Teeuw, R.M., 2002. Application of Geographic Information Systems and Remote Sensing in River Studies. Backhuys Publishers, Leiden.

Llewellyn, G.M., Kooistra, L., Curran, P.J., 2001, The red-edge of soil contaminated grassland. In: Proceedings, 8th International Symposium on Physical Measurements and Signatures in Remote Sensing, Aussois, 8–12 January 2001. CNES, Toulouse, pp. 381–386.

Malley, D.F., Williams, P.C., 1997. Use of near-infrared reflectance spectroscopy in prediction of heavy metals in freshwater sediment by their association with organic matter. Environmental Science and Technology 31, 3461–3467.

Mathworks Inc, 2001. Using Matlab: Version 5.3. The Mathworks Inc, Natick, MA, USA.

Middelkoop, H., 1997. Embanked Floodplains in the Netherlands. Geomorphological Evolution of Various Time Scales. PhD Thesis, Utrecht University, The Netherlands.

Middelkoop, H., 2000. Heavy metal pollution of the river Rhine and Meuse floodplains in the Netherlands. Netherlands Journal of Geosciences 79, 411–427.

Miller, J.R., Hare, E.W., Wu, J., 1990. Quantitative characterisation of the vegetative red edge reflectance. 1. An Inverted-Gaussian reflectance model. International Journal of Remote Sensing 11, 1755–1773.

Miller, J.R., Wu, J., Boyer, M.G., Belanger, M., Hare, E.W., 1991. Seasonal patterns in leaf reflectance red-edge characteristics. International Journal of Remote Sensing 12, 1509–1523.

Milton, N.M., Mouat, D.A., 1989. Remote sensing of vegetation responses to natural and cultural environmental conditions. Photogrammetric Engineering and Remote Sensing 55, 1167–1173.

Mohammed, G.H., Noland, T.L., Irving, D., Sampson, P.H., Zarco-Tejada, P.J., Miller, J.R., 2000. Natural and Stress-Induced Effects on Leaf Spectral Reflectance in Ontario Species. Forest Research Report No. 156, Ontario Ministry of Natural Resources, Canada.

Mohaupt, V., Siber, U., Van den Roovaart, J., Verstappen, C.G., Langenfeld, F., Braun, M., 2001. Diffuse sources of heavy metals in the Rhine basin. Water Science and Technology 44, 41–49.

Reeves III, J., McCarty, G., Mimmo, T., 2002. The potential of diffuse reflectance spectroscopy for the determination of carbon inventories in soils. Environmental Pollution 116, S277–S284.

Richardson, A.J., Everitt, J.H., 1992. Using spectral vegetation indices to estimate rangeland productivity. Geocarta International 1, 63–69.

Schouten, C.J.J., Rang, M.C., De Hamer, B.A., Van Hout, H.R.A., 2000. Strongly polluted deposits in the Meuse river floodplain and their effects on river management. In: Smits, A.J.M., Nienhuis, P.H., Leuven, R.S.E.W. (Eds.), New Approaches to River Management. Backhuys Publishers, Leiden, pp. 33–50.

Sommer, S., Hill, J., Megier, J., 1998. The potential of remote sensing for monitoring rural land use changes and their effects on soil conditions. Agriculture Ecosystems and Environment 67, 197–209.

Van der Perk, J.C., 1996. Afferdensche en Deestsche Waarden. Inrichtingsplan. Ministerie van Verkeer en Waterstaat, Directoraat-Generaal Rijkswaterstaat, RIZA Nota nr. 96.054, Arnhem (in Dutch).

Verkleij, J.A.C., 1994. Effects of heavy metals, organic substances, and pesticides on higher plants. In: Donker, M.H., Eijsackers, H., Heimbach, F. (Eds.), Ecotoxicology of Soil Organisms. Lewis Publishers, Boca Raton, pp. 139–161.